



Cite this: *CrystEngComm*, 2019, 21, 765

Alkali metal salts of 3,6-dinitramino-1,2,4,5-tetrazine: promising nitrogen-rich energetic materials†

Tianhe Zhang,  Jiang Du, Zhimin Li, Xinyu Lin, Lin Wang, Li Yang  and Tonglai Zhang *

The alkali metal salts of 3,6-dinitramino-1,2,4,5-tetrazine (DNAT, **1**), $\text{Li}_2(\text{H}_2\text{O})_4(\text{DNAT})$ (**2**), $\text{Na}_2(\text{H}_2\text{O})_3(\text{DNAT})$ (**3**), $\text{K}_2(\text{H}_2\text{O})(\text{DNAT})$ (**4**), $\text{Rb}_2(\text{DNAT})$ (**5**) and $\text{Cs}_2(\text{DNAT})$ (**6**) were synthesized and characterized by elemental analysis, IR spectroscopy, differential scanning calorimetry (DSC), thermogravimetric analysis (TGA), and single-crystal X-ray diffraction. All of these alkali metal salts possess higher thermal stability (from 240.9 °C to 260.0 °C) than that of DNAT substrate (108.3 °C) due to their numerous coordination bonds and the three-dimensional network structures of the complexes. The number of coordination water molecules, the atomic radius of metal and the different packing forms of the crystal structure contribute to the different thermal stabilities of the alkali metal salts. The experimental (constant-volume) energy of combustion values range from 1331 to 1531 kJ mol⁻¹. The compounds **1**, **4**, **5**, and **6** are sensitive to impact and friction.

Received 25th October 2018,
Accepted 7th December 2018

DOI: 10.1039/c8ce01827h

rs.li/crystengcomm

Introduction

Recently, nitrogen-rich 1,2,4,5-tetrazine-based energetic materials have attracted considerable interest as explosives,¹ propellants² and gas-generating ingredients in automobile airbags.³ In the area of energetic materials, tetrazine with its derivatives could greatly meet the requirements of high nitrogen content and oxygen balance, which makes them desirable as new high-energy-density materials (HEDMs).^{4–9} High-nitrogen energetic materials have become a hot topic in the recent research of HEDMs because of their high energy output and environmental compatibility.

Tetrazine derivatives are of emphases for the research of high energy density energetic materials because of their high nitrogen content. Numerous 1,2,4,5-tetrazine-based energetic materials have been fabricated in recent years, such as 3,3'-azobis (6-amino-1,2,4,5-tetrazine) (DAAT),¹⁰ 3,6-bis(1*H*-1,2,3,4-tetrazol-5-ylamino)-*s*-tetrazine (BTATz),¹¹ 3,6-di(azido)-1,2,4,5-tetrazine (DIAT),¹ 3,6-diguanidino-1,2,4,5-tetrazine (DGTz),¹² 3,6-diamino-1,2,4,5-tetrazine (DAT),¹³ 3,6-dihydeazino-1,2,4,5-tetrazine (DHT)¹⁴ and 3,6-bis-nitroguanyl-1,2,4,5-tetrazine (DNGTz).¹⁵ These compounds have been suggested as potential energetic materials. DNAT has high density, and its oxy-

gen balance approaches zero, which makes DNAT a prospective energetic material (Fig. 1).

DNAT was first discovered by Z. Xizeng and T. Ye.¹⁶ Then, Fischer *et al.*¹⁷ yielded DNAT by the diazotation of 3,5-diamino-1-nitroguanidinium chloride with sodium nitrite. Rudakov *et al.*¹⁸ synthesized DNAT by the reaction of 3,6-diamine-1,2,4,5-tetrazine with 98% HNO₃. Although DNAT has been known for a long time, its crystal structure has not

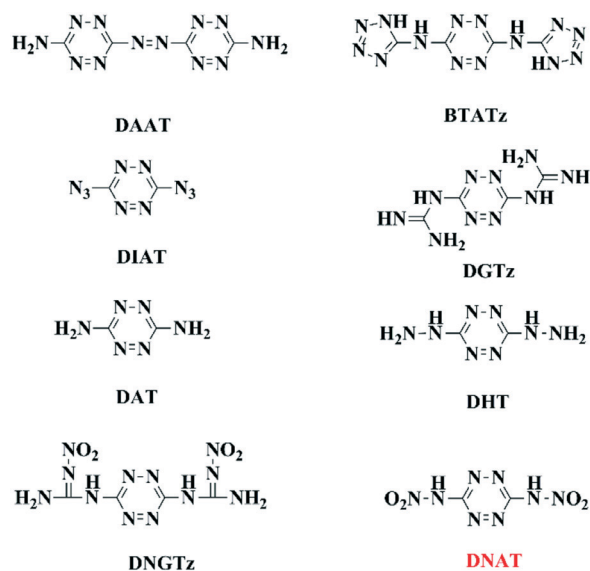


Fig. 1 Molecular structures of 1,2,4,5-tetrazine-based energetic materials.

State Key Laboratory of Explosion Science and Technology, Beijing Institute of Technology, Beijing 100081, China. E-mail: ztlbit@bit.edu.cn;
Fax: +86 10 68911202; Tel: +86 10 68911202

† Electronic supplementary information (ESI) available. CCDC 1567025, 1832596–1832599 and 1858066. For ESI and crystallographic data in CIF or other electronic format see DOI: 10.1039/c8ce01827h

been reported so far, which is necessary to confirm its nature. The oxidative deterioration and high sensitivities of DNAT limit its wide application, which impels us to stabilize DNAT in its alkali metal salts.

Herein, we report the crystal structures of DNAT and its alkali metal salts. Characterizations of these compounds were performed using elemental, IR, DSC, TGA and single-crystal X-ray diffraction analyses. The energetic performances and sensitivities were tested to assess their potential application as energetic materials.

Experimental section

Caution! Although none of the compounds described herein have exploded or detonated over the course of this research, they should be handled in small amounts with extreme care using the appropriate standard safety precautions.

Crystals suitable for X-ray diffraction measurement were obtained as described in the Experimental section. Data were collected on a Rigaku AFC-10/Saturn 724⁺ CCD diffractometer. All of the crystals were irradiated with graphite monochromated Mo K α radiation ($\lambda = 0.71073 \text{ \AA}$) at 153(2) K by the multi-scan mode. All of the structures were solved using the direct methods of SHELXS-97 (ref. 19) and refined by using full-matrix least-squares procedures on F^2 with SHELXL-97.²⁰ All non-hydrogen atoms were obtained from the difference Fourier map and refined anisotropically. Hydrogen atoms were generated geometrically, assigned appropriated isotropic thermal parameters, and included in the structure factor cal-

culations. The crystallographic data and experimental details of structural analysis are summarized in Table 1.

Elemental analyses were performed on a Flash EA 1112 fully automatic trace element analyzer. On a Bruker Equinox 55 infrared spectrometer, IR spectra were recorded from 400 to 4000 cm^{-1} with a resolution of 4 cm^{-1} using KBr pellets. Thermal decomposition behaviours were investigated by performing DSC on a CDR-4 (Shanghai Precision & Scientific Instrument Co., Ltd.) at a heating rate of 10 $^\circ\text{C min}^{-1}$. TG-DTG curves were obtained through a Perkin-Elmer Pyris-1 thermogravimetric analyzer in N_2 at a heating rate of 10 $^\circ\text{C min}^{-1}$. The experimentally determined constant-volume energies of combustion were tested by a Parr-6200 bomb calorimeter (static jacket) with a 6510 water handling system. The calorimeter was calibrated by the combustion of certified benzoic acid (about 1000 mg per pellet) in oxygen atmosphere at a pressure of 3.05 MPa. The samples (about 200 mg each) were prepared and placed in combustion pots, which were subsequently burned in 3.05 MPa atmosphere of pure oxygen.

Synthesis of DNAT (1)

3,6-Diamine-1,2,4,5-tetrazine was prepared according to the published literature reports.¹⁰ Initially, 1 g of 3,6-diamine-1,2,4,5-tetrazine was put into 5 mL of fuming nitric acid at 0 $^\circ\text{C}$, followed by gradual stirring for 1 h. The formed yellow precipitate was recrystallized from ethyl acetate after filtration and drying, yielding 1.53 g of DNAT (85.0%). Crystals

Table 1 X-ray crystallographic data for 1 to 6

| | 1 | 2 | 3 | 4 | 5 | 6 |
|--|--|---|---|--|---|---|
| Formula | $\text{C}_2\text{H}_2\text{N}_8\text{O}_4$ | $\text{C}_2\text{H}_8\text{Li}_2\text{N}_8\text{O}_8$ | $\text{C}_2\text{H}_6\text{Na}_2\text{N}_8\text{O}_7$ | $\text{C}_2\text{H}_2\text{K}_2\text{N}_8\text{O}_5$ | $\text{C}_2\text{Rb}_2\text{N}_8\text{O}_4$ | $\text{C}_2\text{Cs}_2\text{N}_8\text{O}_4$ |
| M (g mol^{-1}) | 202.12 | 286.04 | 300.13 | 296.32 | 371.04 | 465.92 |
| Cryst. syst. | Orthorhombic | Monoclinic | Monoclinic | Orthorhombic | Monoclinic | Triclinic |
| Space group | <i>Pbca</i> | <i>C2/c</i> | <i>C2</i> | <i>Pnna</i> | <i>C2/c</i> | <i>P1</i> |
| a (\AA) | 9.4039(19) | 6.1408(12) | 8.8499(18) | 24.506(5) | 9.1059(18) | 5.3925(11) |
| b (\AA) | 7.8696(16) | 14.773(3) | 12.469(3) | 8.0284(16) | 11.496(2) | 7.3559(15) |
| c (\AA) | 9.4732(19) | 11.457(2) | 6.0807(12) | 4.7044(9) | 9.1102(18) | 7.4275(15) |
| α (deg) | 90 | 90 | 90 | 90 | 90 | 61.64(3) |
| β (deg) | 90 | 100.56(3) | 129.15(3) | 90 | 110.86(3) | 87.56(3) |
| γ (deg) | 90 | 90 | 90 | 90 | 90 | 69.50(3) |
| V (\AA^3) | 701.1(2) | 1021.8(4) | 520.3(2) | 925.5(3) | 891.2(3) | 240.11(11) |
| Z | 4 | 4 | 2 | 4 | 4 | 1 |
| ρ (g cm^{-3}) | 1.915 | 1.859 | 1.916 | 2.127 | 2.765 | 3.222 |
| T (K) | 153.15 | 153.15 | 153.15 | 153.15 | 153.15 | 153.15 |
| $F(000)$ | 408.0 | 584.0 | 304.0 | 592.0 | 696.0 | 210.0 |
| μ (mm^{-1}) | 0.177 | 0.176 | 0.247 | 1.056 | 11.001 | 7.609 |
| Reflns. collected | 4220 | 3907 | 1727 | 6346 | 2888 | 1617 |
| Indep. reflns. | 786 | 1160 | 890 | 1044 | 1013 | 922 |
| Params. | 64 | 91 | 87 | 79 | 74 | 73 |
| R_{int} | 0.0392 | 0.0236 | 0.0204 | 0.0373 | 0.0765 | 0.0622 |
| S | 1.230 | 1.083 | 1.067 | 1.166 | 1.237 | 1.085 |
| R_1 ($I > 2\sigma(I)$) ^a | 0.0606 | 0.0303 | 0.0205 | 0.0356 | 0.0442 | 0.0394 |
| R_1 (all data) | 0.0640 | 0.0307 | 0.0205 | 0.0360 | 0.0513 | 0.0398 |
| wR_2 ($I > 2\sigma(I)$) ^a | 0.1389 | 0.0762 | 0.0545 | 0.0881 | 0.0984 | 0.0966 |
| wR_2 (all data) | 0.1402 | 0.0764 | 0.0545 | 0.0884 | 0.1042 | 0.0970 |
| CCDC | 1567025 | 1832599 | 1832596 | 1832597 | 1832598 | 1858066 |

^a $R_1 = \sum ||F_o| - |F_c|| / \sum |F_o|$. $wR_2 = [\sum w(F_o^2 - F_c^2)^2 / \sum w(F_o^2)^2]^{1/2}$; $w = 1/[\sigma^2(F_o^2) + (xP)^2 + yP]$.

suitable for single X-ray diffraction were obtained through slow evaporation in ethyl acetate solution. T_{dec} : 106.4 °C. IR (KBr): 3864, 3742, 3675, 3618, 3167, 3032, 2897, 2669, 2312, 1669, 1596, 1480, 1424, 1324, 1216, 1087, 962, 901, 788, 744, 700, 487. Anal. calcd. for $\text{C}_2\text{H}_2\text{N}_8\text{O}_4$ (MW 202.12): C, 11.88; H, 1.00; N, 55.44. Found: C, 11.83; H, 0.99; N, 55.41.

Synthesis of $\text{Li}_2(\text{H}_2\text{O})_4(\text{DNAT})$ (2)

$\text{LiOH}\cdot\text{H}_2\text{O}$ (42.0 mg, 1.0 mmol) was added into a solution of DNAT (0.5 mmol, 101.0 mg in 5 mL of methanol) with stirring at 25 °C. After 30 min, a red solution formed. The red crystal of 2 was cultured suitable for X-ray structural determination through slow evaporation in solution. Yield: 96 mg (67.1%). T_{dec} : 250.4 °C. IR (KBr): 3466, 2190, 1719, 1664, 1560, 1543, 1488, 1384, 1278, 1083, 1041, 770, 592. Anal. calcd. for $\text{Li}_2\text{C}_2\text{H}_8\text{N}_8\text{O}_8$ (MW 286.04): C, 8.40; H, 2.82; N, 39.18. Found: C, 8.52; H, 2.63; N, 39.36.

Synthesis of $\text{Na}_2(\text{H}_2\text{O})_3(\text{DNAT})$ (3)

NaOH (40.0 mg, 1.0 mmol) was added into a solution of DNAT (0.5 mmol, 101.0 mg in 5 mL of methanol) with stirring at 25 °C. After 30 min, a red precipitate formed, which was filtered, washed with a small amount of methanol and dried (yield: 112 mg, 74.6%). Crystals suitable for single X-ray diffraction could be obtained through slow evaporation in methanol solution. T_{dec} : 260.0 °C. IR (KBr): 3505, 3416, 2925, 2375, 2339, 2165, 1631, 1467, 1415, 1364, 1297, 1073, 949, 883, 767, 575, 525. Anal. calcd. for $\text{Na}_2\text{C}_2\text{H}_6\text{N}_8\text{O}_7$ (MW 300.13): C, 8.00; H, 2.02; N, 37.34. Found: C, 8.32; H, 2.21; N, 37.62.

Synthesis of $\text{K}_2(\text{H}_2\text{O})(\text{DNAT})$ (4)

The synthesis method for compound 4 was similar to that of 3 except 1 mmol of KOH was used instead of 1 mmol of NaOH . Crystals suitable for single X-ray diffraction could be obtained through slow evaporation in methanol solution. Yield: 117 mg (80.0%). T_{dec} : 253.7 °C. IR (KBr): 3448, 1638, 1544, 1406, 1270, 1074, 1042, 942, 869, 773, 752, 571, 521. Anal. calcd. for $\text{K}_2\text{C}_2\text{H}_2\text{N}_8\text{O}_5$ (MW 296.32): C, 8.11; H, 0.68; N, 37.82. Found: C, 8.24; H, 0.84; N, 38.02.

Synthesis of $\text{Rb}_2(\text{DNAT})$ (5)

The synthesis method for compound 5 was similar to that of 3 except 0.5 mmol of Rb_2CO_3 was used instead of 1 mmol of NaOH . Crystals suitable for single X-ray diffraction could be obtained through slow evaporation in its solution of methanol. Yield: 122 mg (65.8%). T_{dec} : 246.0 °C. IR (KBr): 3422, 2923, 2696, 2362, 2344, 2271, 1846, 1773, 1618, 1560, 1543, 1491, 1258, 1066, 1037, 940, 867, 771, 749, 567, 519. Anal. calcd. for $\text{Rb}_2\text{C}_2\text{N}_8\text{O}_4$ (MW 371.04): C, 6.47; N, 30.20. Found: C, 7.12; N, 31.03.

Synthesis of $\text{Cs}_2(\text{DNAT})$ (6)

The synthesis method for compound 6 was similar to that of 3 except 0.5 mmol of Cs_2CO_3 was used instead of 1 mmol of

NaOH . Crystals suitable for single X-ray diffraction could be obtained through slow evaporation in methanol solution. Yield: 175 mg (75.1%). T_{dec} : 240.9 °C. IR (KBr): 3423, 2922, 2684, 2265, 1847, 1618, 1560, 1543, 1403, 1260, 1066, 1035, 938, 865, 771, 746, 576, 519. Anal. calcd. for $\text{Cs}_2\text{C}_2\text{N}_8\text{O}_4$ (MW 465.88): C, 5.16; N, 24.05. Found: C, 5.17; N, 23.94.

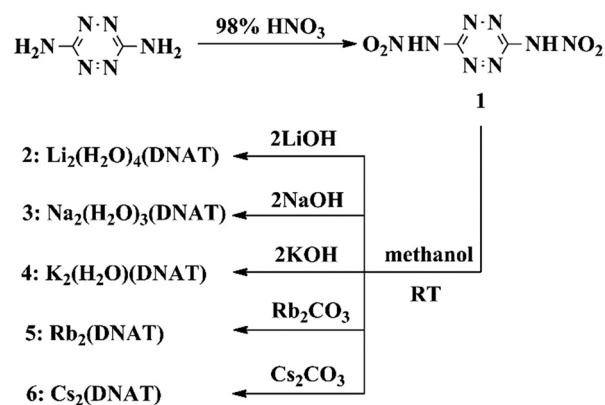
Results and discussion

DNAT was prepared by the reaction of 3,6-diamine-1,2,4,5-tetrazine with 98% HNO_3 according to the published literature reports.^{13,18} All other chemicals were pure analytical-grade materials obtained commercially and used as received. As a nitrogen-rich tetrazine, DNAT is a potential ligand for coordinating with metal cations. Alkali metal salts were synthesized for the sake of “green” metal energetic complexes. As shown in Scheme 1, all of the salts were synthesized in a straightforward manner. The compounds were prepared *via* a neutralization reaction and a metathetical reaction.

The molecular structure of DNAT was confirmed by single-crystal X-ray diffraction. DNAT crystallized in the orthorhombic space group *Pbca* with four molecular moieties in each unit cell, a density of 1.915 g cm^{-3} , and a unit cell volume of 701.1 (2) \AA^3 (Table 1). In the DNAT molecule, the interatomic distances of C1–N2, C1–N3, C1–N4 and N3–N4 bonds are 1.393(3), 1.337(3), 1.337(3), 1.323(3) \AA , respectively. These bonds are longer than a C=N double bond or a N=N double bond, but shorter than a C–N single bond or a N–N single bond, which suggests that some multiple bond character is present. In addition, the torsion angles show that the tetrazine ring and amino group in DNAT are coplanar. Moreover, the two nitro groups have a certain angle of distortion and are centrally symmetric.

Compounds 2 to 4 are simple salts of DNAT with chelated water molecules, while compounds 5 and 6 have no chelated water molecules. Their formulae can be expressed as $\text{Li}_2(\text{H}_2\text{O})_4(\text{DNAT})$ (2), $\text{Na}_2(\text{H}_2\text{O})_3(\text{DNAT})$ (3), $\text{K}_2(\text{H}_2\text{O})(\text{DNAT})$ (4), $\text{Rb}_2(\text{DNAT})$ (5), and $\text{Cs}_2(\text{DNAT})$ (6).

Compounds 2 and 5 crystallize in the monoclinic space group *C2/c*, compound 3 crystallizes in the monoclinic space



Scheme 1 Syntheses of 3,6-dinitramino-1,2,4,5-tetrazine (DNAT) and salts 2 to 6.

group C_2 , compound 4 crystallizes in the orthorhombic space group $Pnna$, and compound 6 has triclinic ($P\bar{1}$) symmetry. Compound 2 has four coordinated water molecules, compound 3 has three coordinated water molecules, compound 4 has one coordinated water molecule and there are no coordinated water molecules in compounds 5 and 6. Because of the increase in the relative molecular mass of metal cations, the densities of energetic salts increase.

Several water molecules are found coordinated to the central ions (four to the $\text{Li}(i)$ ion, three to the $\text{Na}(i)$ ion and one to the $\text{K}(i)$ ion). In compound 2, each $\text{Li}(i)$ cation is six-coordinate. The distorted octahedral complex consists of a lithium atom bonded to four water molecules and a DNAT anion (*viz.*, Li-O3 (water molecule) $\times 2$, Li-O4 (water molecule) $\times 2$, Li-O2 (DNAT), and Li-N2 (DNAT)). All of the water molecules are bridging ligands. In compound 3, each $\text{Na}(i)$ cation is seven-coordinate. The sodium atom coordinates with three water molecules and two DNAT anions (*viz.*, Na-O1 (water molecule), Na-O2 (water molecule) $\times 2$, Na-O3 (DNAT), Na-N2 (DNAT), Na-N3 (DNAT), and Na-N4 (DNAT)). In the molecules of 4, the $\text{K1}(i)$ cation is ten-coordinate. The $\text{K1}(i)$ cation coordinates with six DNAT anions (*viz.*, K1-O1 (DNAT) $\times 2$; K1-O2 (DNAT) $\times 6$; K1-N1 (DNAT) $\times 2$). The $\text{K2}(i)$ cation is six-coordinate. The $\text{K2}(i)$ cation coordinates with two water molecules and three DNAT anions (*viz.*, K2-O1 (DNAT) $\times 2$, K2-O3 (water molecule) $\times 2$, and K2-N2 (DNAT) $\times 2$). In compound 5, the $\text{Rb1}(i)$ cation is eight-coordinate, coordinating with six DNAT anions, while the $\text{Rb2}(i)$ cation is ten-coordinate, coordinating with six DNAT anions. In compound 6, each $\text{Cs}(i)$ cation is thirteen-coordinate, coordinating with six DNAT anions. With the increase in atomic radius of the

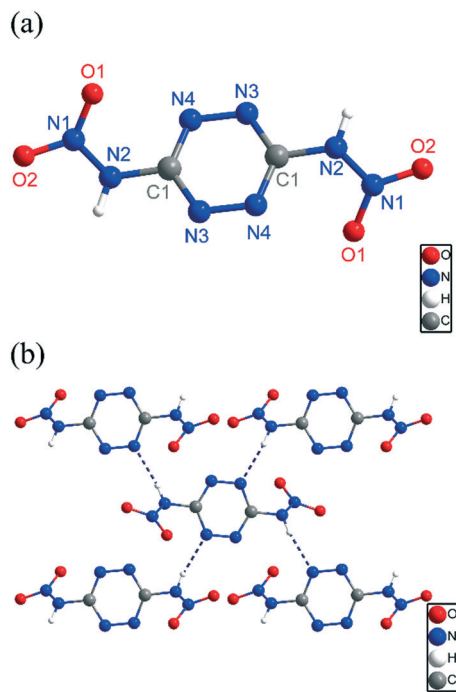


Fig. 2 (a) Molecular structure of 1 and its labelling scheme. (b) The packing diagram of compound 1 viewed along the c -axis.

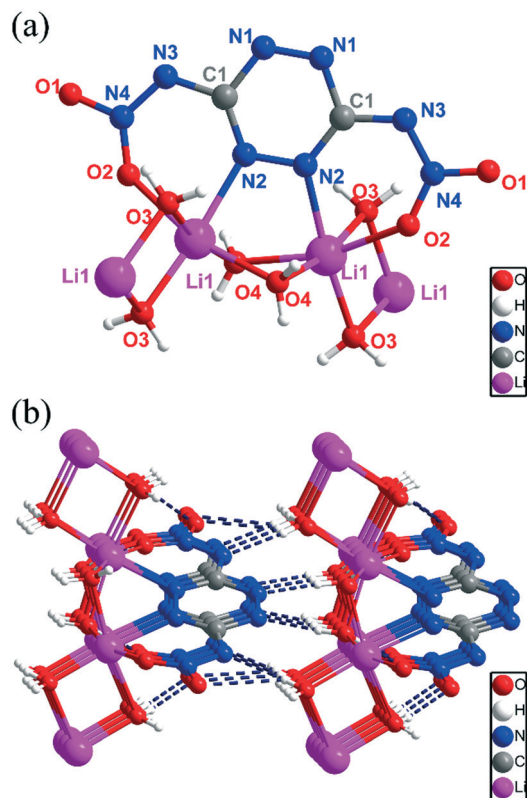


Fig. 3 (a) Molecular structure of 2 and its labelling scheme. (b) The packing diagram of compound 2 viewed along the a -axis.

metal, the coordination number increases, and the coordination bond lengths become longer (M-N , 2.151 Å to 3.671 Å; M-O , 2.287 Å to 3.275 Å; M , metal atom).

As shown in Fig. 2b–7b, the packing structures of the compounds are different. The packing structure of 1 was built up and linked to a 2D layer by various hydrogen bonds, as shown along the c -axis in Fig. 2b. The tetrazine rings of DNAT are in the same plane, and the nitro-groups are on different sides of the plane. Each DNAT molecule forms hydrogen bonds cross-linked with four neighboring DNAT molecules. The packing structures of 2 to 6 were built up and linked into the 3D network by various hydrogen bonds and water molecules, as shown in Fig. 3b–7b. As shown in Fig. 3b and S4,[†] a series of energetic molecules stack in a wave-like mode to form an energetic layer. Adjacent layers were linked by hydrogen bonds. Each DNAT molecule coordinates with two lithium cations and forms eight hydrogen bonds with water molecules. In compound 3, adjacent layers were linked by water molecules and hydrogen bonds (Fig. S6[†]). Each DNAT molecule coordinates with four sodium cations and forms six hydrogen bonds with water molecules (Fig. 4b). As for compounds 4 to 6, the energetic layers were linked with metal layers by coordination bonds (Fig. S8, S10 and S12[†]). For compound 4, each DNAT molecule coordinates with six potassium cations and forms two hydrogen bonds with water molecules (Fig. 5b). As for compound 5, each DNAT molecule coordinates with twelve rubidium cations (Fig. 6b). In

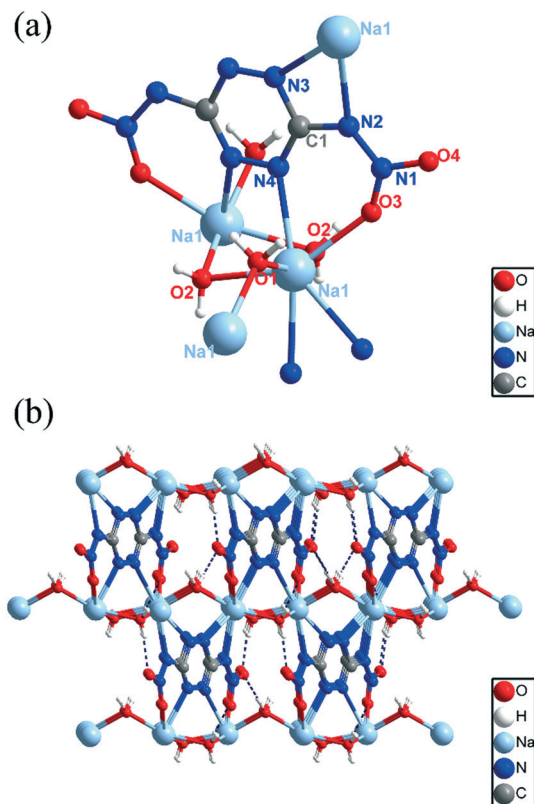


Fig. 4 (a) Molecular structure of **3** and its labelling scheme. (b) The packing diagram of compound **3** viewed along the *c*-axis.

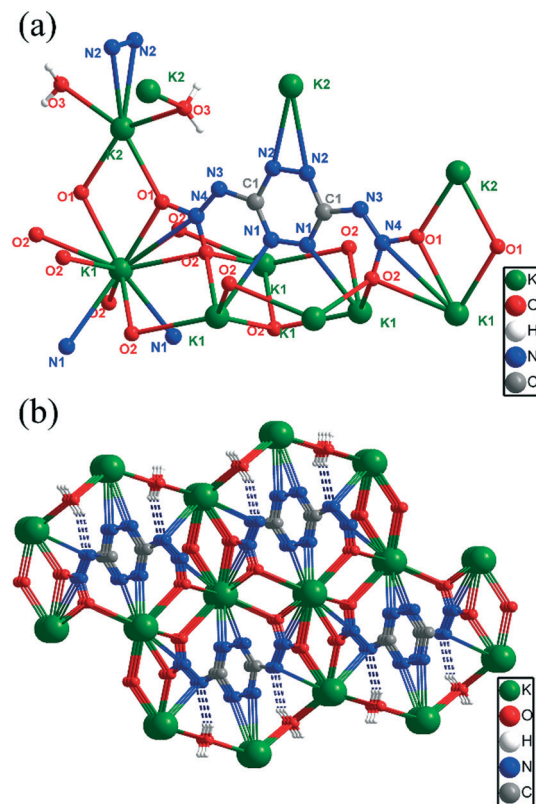


Fig. 5 (a) Molecular structure of **4** and its labelling scheme. (b) The packing diagram of compound **4** viewed along the *c*-axis.

compound **6**, each DNAT molecule coordinates with six cesium cations (Fig. 7b).

Physicochemical properties

The physicochemical properties of **1** to **6** are summarized in Table 5. Density is one of the most important properties of energetic materials. The densities of compounds **1** to **6** range between 1.859 g cm^{-3} (**2**) and 3.222 g cm^{-3} (**6**) (Table 5), which are mainly affected by the alkalis. The nitrogen content of DNAT is 55.41%, which is higher than that of RDX, HMX, and CL-20. The OBs of all compounds range from -3.43% (**6**) to -7.92% (**1**), which almost approach zero oxygen balance.

Thermal analyses

The thermal stabilities of compounds **1** to **6** were investigated by using DSC and TGA techniques. The dehydration and decomposition temperatures were determined by DSC measurements, which were performed on a CDR-4 (Shanghai Precision & Scientific Instrument Co., Ltd.) calibrated by standard pure indium, tin and zinc at a heating rate of $10 \text{ }^\circ\text{C min}^{-1}$. It can be seen that the decomposition temperatures of these compounds range from $108.3 \text{ }^\circ\text{C}$ to $260.0 \text{ }^\circ\text{C}$. The decomposition temperatures of all of the salts are nearly comparable to that of RDX ($230 \text{ }^\circ\text{C}$) and lower than that of HMX ($287 \text{ }^\circ\text{C}$). In compound **2**, only two N atoms of each tetrazine ring coordinate with the metal atoms. Moreover, all the N atoms of each tetrazine ring

coordinate with the metal atoms of the other alkali metal salts. Hence, compound **2** does not obey the law of thermodynamics. Additionally, according to the TG-DTG curves, there are two distinct mass loss processes observed for DNAT. One occurs from $108.1 \text{ }^\circ\text{C}$ to $158.6 \text{ }^\circ\text{C}$, corresponding to a mass loss of 49.8%, and the other occurs from $158.6 \text{ }^\circ\text{C}$ to $186.0 \text{ }^\circ\text{C}$, corresponding to a mass loss of 27.2%. The first mass loss of 49.8% might correspond to the decomposition loss of the nitramino groups ($-\text{NH}-\text{NO}_2$). There was no residue after $281.3 \text{ }^\circ\text{C}$, which indicates that the compound totally decomposed at $281.3 \text{ }^\circ\text{C}$ into gaseous products. Other compounds have corresponding processes of dehydration and thermal decomposition; the final products are corresponding carbonates.

The thermal decomposition activation energy and pre-exponential factor have been calculated by using Kissinger's method²¹ and Ozawa's method²² (Table 2), both of which were on the basis of the first exothermic decomposition peak temperatures tested at different heating rates (Table S35[†]). The Kissinger equation and Ozawa's equation are listed as (1) and (2), respectively:

$$\ln \beta/T_p = \ln AR/E_K + E_K/RT_p \quad (1)$$

$$\lg \beta = \lg AE_O/G(\alpha)R - 0.4567E_O/RT_p - 2.315 \quad (2)$$

where T_p is the peak temperature (K), R is the gas constant ($8.314 \text{ J K}^{-1} \text{ mol}^{-1}$), β is the linear heating rate (K min^{-1}), and

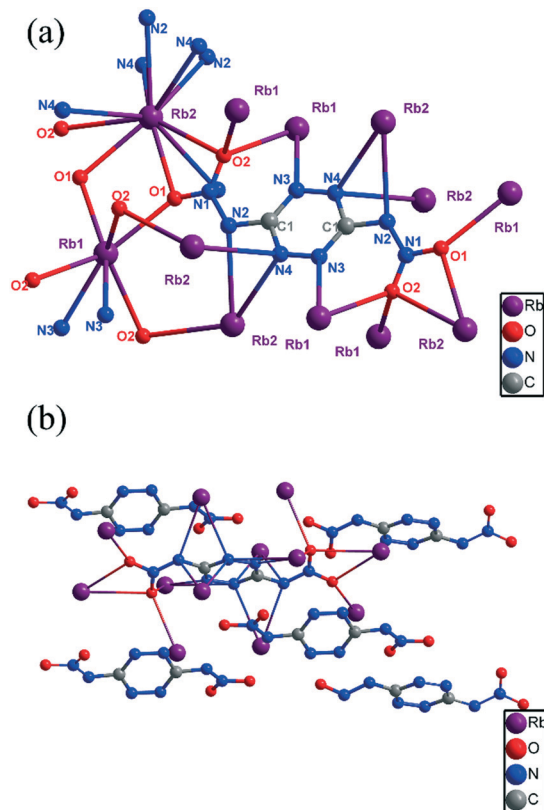


Fig. 6 (a) Molecular structure of 5 and its labelling scheme. (b) The packing diagram of compound 5 viewed along the *a*-axis.

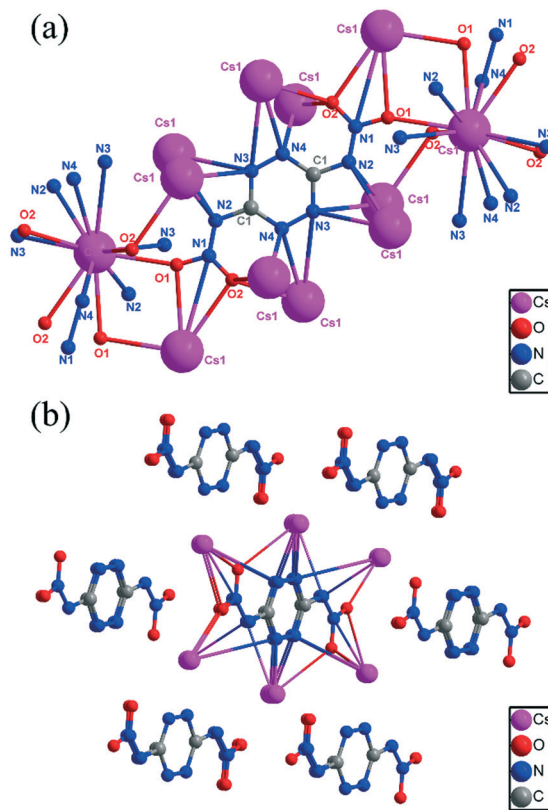


Fig. 7 (a) Molecular structure of 6 and its labelling scheme. (b) The packing diagram of compound 6 viewed along the *a*-axis.

$G(\alpha)$ is the reaction mechanism function. The measured peak temperatures to one decimal place as well as the energetic nature of the compound determine the four significant parameters as listed in Table 2, and the standard errors (S) are acceptable. As shown in Table 2, with the increase in atomic radius of the metal, the activation energy and pre-exponential factor of compounds decrease significantly. The activation energy and pre-exponential factor of DNAT are higher than those of DGTz²³ and DHT.²⁴

The values of the peak temperature corresponding to $\beta \rightarrow 0$ (T_{p0}), the corresponding critical temperature of thermal explosion (T_b), the entropy of activation (ΔS^\ddagger), the enthalpy of activation (ΔH^\ddagger), and the free energy of activation (ΔG^\ddagger) are obtained and listed in Table 3 according to equations reported by Zhang *et al.*²⁵ The equations for calculating are listed as (3) to (7), severally:

$$T_{pi} = T_{p0} + a\beta + b\beta^2 + c\beta^3 \quad (3)$$

$$T_b = \left(E_K - \sqrt{E_K^2 - 4E_K RT_{p0}} \right) / 2R \quad (4)$$

$$A = (k_B T_{p0} / h) \exp(1 + \Delta S^\ddagger / R) \quad (5)$$

$$\Delta H^\ddagger = E_K - RT_{p0} \quad (6)$$

$$\Delta G^\ddagger = \Delta H^\ddagger - T_{p0} \Delta S^\ddagger \quad (7)$$

where a , b and c are coefficients, k_B is the Boltzmann constant ($1.381 \times 10^{-23} \text{ J K}^{-1}$) and h is the Planck constant ($6.626 \times 10^{-34} \text{ J s}$).

As shown in Table 3, with the increase in atomic radius of the metal, the entropy of activation and enthalpy of activation decrease significantly. The enthalpy of activation and free energy of activation of the compounds are all greater than 0, which indicates that the thermal decomposition process is a non-spontaneous endothermic process.

The thermal sensitivities of the six samples were studied with 5 s delay bursting point tests (Table S36[†]), and the results are listed in Table 4. The equations for calculating the 5 s delay time are listed as (8) and (9):

Table 2 Non-isothermal reaction kinetics parameters of compounds 1 to 6

| Compound | Kissinger's method | | | Ozawa's method | |
|----------|--------------------------|-----------|-------|--------------------------|-------|
| | $E_K/\text{kJ mol}^{-1}$ | $\lg A_K$ | R_K | $E_O/\text{kJ mol}^{-1}$ | R_O |
| 1 | 366.7 | 48.9 | 0.99 | 354.8 | 0.99 |
| 2 | 333.7 | 31.7 | 0.99 | 325.6 | 0.99 |
| 3 | 213.1 | 19.0 | 0.98 | 211.0 | 0.98 |
| 4 | 139.6 | 11.8 | 0.99 | 141.1 | 0.99 |
| 5 | 122.5 | 10.3 | 0.98 | 124.6 | 0.98 |
| 6 | 92.7 | 7.2 | 0.99 | 96.4 | 0.99 |

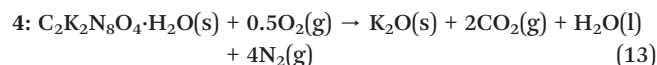
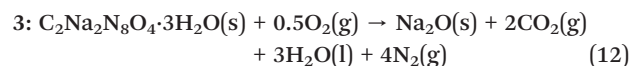
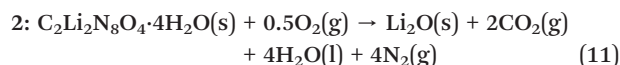
Table 3 Calculation of the critical temperatures of thermal explosion, ΔS^\ddagger , ΔH^\ddagger and ΔG^\ddagger

| Compound | T_{p0}/K | T_b/K | $\Delta S^\ddagger/J K^{-1} mol^{-1}$ | $\Delta H^\ddagger/kJ mol^{-1}$ | $\Delta G^\ddagger/kJ mol^{-1}$ |
|----------|------------|---------|---------------------------------------|---------------------------------|---------------------------------|
| 1 | 378.5 | 381.8 | 689.0 | 363.6 | 102.8 |
| 2 | 507.4 | 513.9 | 357.9 | 329.5 | 147.9 |
| 3 | 524.2 | 535.3 | 114.9 | 208.7 | 148.5 |
| 4 | 506.2 | 522.4 | -22.8 | 135.4 | 147.0 |
| 5 | 484.5 | 501.5 | -51.4 | 118.5 | 143.4 |
| 6 | 495.9 | 520.1 | -110.9 | 88.6 | 143.6 |

T_{p0} : peak temperature corresponding to $\beta \rightarrow 0$; T_b : critical temperatures of thermal explosion; ΔS^\ddagger : entropy of activation; ΔH^\ddagger : enthalpy of activation; ΔG^\ddagger : free energy of activation.

Table 4 Results of 5 s bursting point tests

| Compound | 1 | 2 | 3 | 4 | 5 | 6 |
|-------------------|-----|-----|-----|-----|-----|-----|
| $T_{5s}/^\circ C$ | 136 | 307 | 299 | 323 | 282 | 306 |



$$\tau = ce^{\frac{E}{RT}} \quad (8)$$

$$\ln \tau = \frac{E}{RT} + \ln c \quad (9)$$

where τ is the value delayed time (s) and c is a constant.

Enthalpy of formation

The enthalpy of formation is a significant characteristic used to assess the energetic properties. The constant-volume energies of combustion ($\Delta_c U$) of these compounds were determined experimentally using oxygen bomb calorimetry. The enthalpy of combustion, $\Delta_c H^\circ$, can be calculated using the formula $\Delta_c H^\circ = \Delta_c U + \Delta nRT$, where Δn is the difference in the number of moles of gases between the products and the reactants. The enthalpies of formation ($\Delta_f H^\circ$) at 298 K were calculated on the basis of the combustion reactions (eqn (10)–(15)) and the Hess thermochemical cycle. The heat of formation of the combustion products ($CO_2(g)$ $-393.5 kJ mol^{-1}$ and $H_2O(l)$ $-285.8 kJ mol^{-1}$) were obtained from the literature.²⁶



The combustion energies of compounds 1 to 6 ($\Delta_c U$) are $-1360 kJ mol^{-1}$ (1), $-1479 kJ mol^{-1}$ (2), $-1331 kJ mol^{-1}$ (3), $-1531 kJ mol^{-1}$ (4), $-1407 kJ mol^{-1}$ (5), and $-1456 kJ mol^{-1}$ (6). The calculated enthalpies of formation of 1 to 6 are $275.9 kJ mol^{-1}$ (1), $-1062.6 kJ mol^{-1}$ (2), $-740.9 kJ mol^{-1}$ (3), $81.2 kJ mol^{-1}$ (4), $267.8 kJ mol^{-1}$ (5), and $309.9 kJ mol^{-1}$ (6). With the increase in atomic radius of the metal, the calculated enthalpies of formation of compounds also increase significantly; the calculated enthalpy of formation of compound 6 is even higher than that of DNAT.

Sensitivities

To assess the stability of the studied compounds, impact and friction sensitivities were determined according to BAM standard methods,^{27,28} and the results were summarized in

Table 5 Physicochemical properties of compounds 1 to 6

| | 1 | 2 | 3 | 4 | 5 | 6 | Pb(N ₃) ₂ |
|-------------------------------|-------|---------|--------|-------|-------|-------|----------------------------------|
| $T_d (^\circ C)^a$ | 108.3 | 250.4 | 260.0 | 253.7 | 246.0 | 240.9 | 315.0 |
| $N (\%)^b$ | 55.41 | 39.16 | 37.32 | 37.80 | 30.19 | 24.05 | 28.9 |
| $\Omega (\%)^c$ | -7.92 | -5.59 | -5.33 | -5.40 | -4.31 | -3.43 | -11.0 |
| $\rho (g cm^{-3})^d$ | 1.915 | 1.859 | 1.916 | 2.127 | 2.765 | 3.222 | 4.8 |
| $-\Delta_c U (kJ mol^{-1})^e$ | 1360 | 1479 | 1331 | 1531 | 1407 | 1456 | — |
| $\Delta_f H (kJ mol^{-1})^f$ | 272.6 | -1062.6 | -740.9 | 81.2 | 267.8 | 309.9 | 450.1 |
| IS (J) ^g | 0.4 | >40 | >40 | 2.96 | 2.88 | 2.80 | 2.5–4.0 |
| FS (N) ^h | 12 | >360 | >360 | 112 | 108 | 192 | 0.1–1 |

^a Decomposition temperature (from DSC, $\beta = 10 ^\circ C min^{-1}$). ^b Nitrogen content. ^c Oxygen balance ($\Omega = (O - 2C - H/2 - xZ) \times 1600/M$); H , number of hydrogen atoms; C , number of carbon atoms; O , number of oxygen atoms; Z , number of metal atoms; M , molecular weight of the compound. Alkali metals: $x = 0.5$. ^d Density, 153.15 K. ^e Experimental (constant-volume) energy of combustion. ^f Calculated energy of formation. ^g Impact sensitivity. ^h Friction sensitivity.

Table 5. On the basis of the UN classification standard of sensitivities,²⁹ compound 1 is very sensitive toward impact and friction (impact = 0.4 J and friction = 12 N). Because of a large amount of coordination water molecules, compound 2 and compound 3 are both insensitive (impact >40 J and friction >360 N). Compounds 4 to 6 are very sensitive toward impact and sensitive toward friction (impact ≤3 J and friction <360 N and >80 N) because of less or no coordination water molecules. Compared to the typical primary explosive Pb(N₃)₂, it is clear that compounds 4, 5 and 6 exhibit similar impact sensitivities and lower friction sensitivities.

Conclusions

In this study, DNAT (1) and its alkali metal salts 2 to 6 were synthesized and fully characterized. The structures of all the compounds were confirmed by single-crystal X-ray diffraction analysis. The densities of all the compounds lie in the range between 1.859 g cm⁻³ (2) and 3.222 g cm⁻³ (6). The energetic salts exhibit better thermal stabilities than DNAT (108.3 °C), with decomposition temperatures ranging from 240.9 to 260.0 °C. All of the energetic compounds show excellent oxygen balance and enthalpies of formation. All the compounds except 2 and 3 are sensitive to impact and friction. These metal DNAT salts may be excellent “green” energetic materials and can be useful as gas generators or additives in solid rockets as low-smoke propellant ingredients since they show promising properties with respect to stability, sensitivity, and energetics.

Conflicts of interest

There are no conflicts to declare.

Acknowledgements

The authors acknowledge the financial support from the National Natural Science Foundation of China (21805008), the State Key Laboratory of Explosion Science and Technology (ZDKT 17-01) and the Fundamental Research Funds for the Central Universities (2017cx10001).

Notes and references

- M. H. V. Huynh, M. A. Hiskey, J. G. Archuleta, E. L. Roemer and R. Gilardi, *Angew. Chem., Int. Ed.*, 2004, **43**, 5658–5661.
- A. N. Ali, S. F. Son, M. A. Hiskey and D. L. Nau, *J. Propul. Power*, 2004, **20**, 120–126.
- H. R. Blomquist, *US Pat.*, 6588797, 2003.
- A. E. Sifain, J. A. Bjorgaard, T. W. Myers, J. M. Veauthier, D. E. Chavez, O. V. Prezhdo, R. J. Scharff and S. Tretiak, *J. Phys. Chem. C*, 2016, **120**, 28762–28773.
- T. M. Klapotke, D. G. Piercey, F. Rohrbacher and J. Stierstorfer, *Z. Anorg. Allg. Chem.*, 2012, **638**, 2235–2242.
- T. Wei, J. Z. Wu, W. H. Zhu, C. C. Zhang and H. M. Xiao, *J. Mol. Model.*, 2012, **18**, 3467–3479.
- Y. H. Luo, C. Chen, D. L. Hong, X. T. He, J. W. Wang and B. W. Sun, *J. Phys. Chem. Lett.*, 2018, **9**, 2158–2163.
- Y.-H. Luo, C. Chen, D.-L. Hong, X.-T. He, J.-W. Wang, T. Ding, B.-J. Wang and B.-W. Sun, *ACS Appl. Mater. Interfaces*, 2018, **10**, 9495–9502.
- Y. H. Luo, X. T. He, D. L. Hong, C. Chen, F. H. Chen, J. Jiao, L. H. Zhai, L. H. Guo and B. W. Sun, *Adv. Funct. Mater.*, 2018, 1804822.
- D. E. Chavez, M. A. Hiskey and R. D. Gilardi, *Angew. Chem., Int. Ed.*, 2000, **39**, 1791–1793.
- D. E. Chavez, M. A. Hiskey and D. L. Naud, *Propellants, Explos., Pyrotech.*, 2004, **29**, 209–215.
- D. E. Chavez, M. A. Hiskey and D. L. Naud, *Propellants, Explos., Pyrotech.*, 2004, **29**, 209–215.
- M. D. Coburn and D. G. Ott, *J. Heterocyclic Chem.*, 1990, **27**, 1941–1945.
- D. E. Chavez and M. A. Hiskey, *J. Heterocyclic Chem.*, 1998, **35**, 1329–1332.
- D. E. Chavez, M. A. Hiskey and R. D. Gilardi, *Org. Lett.*, 2004, **6**, 2889–2891.
- Z. Xizeng and T. Ye, in: *Proceedings of International Symposium Pyrotechnics and Explosives*, China Academic Publishers, Beijing, 1987, p. 241.
- D. Fischer, T. M. Klapoetke and J. Stierstorfer, *New Trends in Research of Energetic Materials, Proceedings of the Seminar*, 15th, Pardubice, Czech Republic, Apr. 18–20, 2012, 2012, pp. 117–129.
- G. F. Rudakov, T. V. Ustinova, I. B. Kozlov and V. F. Zhilin, *Chem. Heterocycl. Compd.*, 2014, **50**, 53–64.
- G. M. Sheldrick, *SHELXS97: Program for Crystal Structure Solution*, University of Göttingen, Göttingen, Germany, 1997.
- G. M. Sheldrick, *SHELXL97: Program for Crystal Structure Refinement*, University of Göttingen, Göttingen, Germany, 1997.
- H. E. Kissinger, *Anal. Chem.*, 1957, **29**, 1702–1706.
- T. Ozawa, *Bull. Chem. Soc. Jpn.*, 1965, **38**, 1881–1886.
- Z. M. Li, S. H. Xie, J. G. Zhang, J. L. Feng, K. Wang and T. L. Zhang, *J. Chem. Eng. Data*, 2012, **57**, 729–736.
- J. G. Zhang, X. Yin, J. T. Wu, M. Sun, J. L. Feng, T. L. Zhang and Z. N. Zhou, *Chin. J. Inorg. Chem.*, 2013, **29**, 2587–2594.
- T. Zhang, R. Hu, Y. Xie and F. Li, *Thermochim. Acta*, 1994, **244**, 171–176.
- D. R. Lide, *Standard Thermodynamic Properties of Chemical Substances*, *CRC Handbook of Chemistry and Physics*, Internet Version 2007, 87th edn, Taylor and Francis, Boca Raton, FL, 2007.
- NATO standardization agreement (STANAG) on explosives, impact-sensitivity tests, no. 4489, 1st edn, September 17, 1999.
- NATO standardization agreement (STANAG) on explosive, friction sensitivity tests, no. 4487, 1st edn, August 22, 2002.
- According to UN recommendations on the transport of dangerous goods, impact: insensitive >40 J, less sensitive ≥35 J, sensitive ≥4 J, very sensitive ≤3 J. Friction: insensitive >360 N, less sensitive = 360 N, 80 N < sensitive <360 N, very sensitive <80 N, extremely sensitive <10 N.